Synthesis and Characterization of Light-Emitting Main-Chain Metallo-Polymers Containing Bis-Terpyridyl Ligands with Various Lateral Substituents

YI-YU CHEN, HONG-CHEU LIN

Department of Materials Science and Engineering, National Chiao Tung University, Hsinchu, Taiwan, Republic of China

Received 16 January 2007; accepted 28 February 2007
DOI: 10.1002/pola.22073
Published online in Wiley InterScience (www.interscience.wiley.com).

ABSTRACT: A series of conjugated monomers (**5a-5d**) with various lateral substituents were symmetrically synthesized by the Sonogashira coupling reaction, in which central aromatic units (i.e. 9,9-dipropylfluorenes) were linked to 2,2′:6′,2′-terpyridyl (tpy) units via phenylene/ethynylene fragments. These light-emitting monomers were further reacted with zinc(II) ions and subsequently anion exchanged to produce supramolecular main-chain metallo-polymers (**6a-6d**). The formation of polymers **6a-6d** was confirmed by the increased viscosities (up to 1.5–1.83 times) relative to those of their analogous monomers. The results of ^{1}H NMR titration and UV-Vis spectral titration revealed a detailed complexation process of metallo-polymers by varying the molar ratios of zinc(II) ions to monomers. After coordination with zinc(II) ions, the luminescent and thermal properties of the polymers were enhanced by the formation of metallo-supramolecular structures in contrast to their monomer counterparts. PLED devices employing these metallo-polymers as emitters gave yellow to orange electroluminescence (EL) emissions with turn-on voltages around 6 V. The maximum power efficiency, external quantum yield, and brightness of the PLED device containing polymer **6c** were 0.33 cd A^{-1} (at 14 V), 1.02%, and 931 cd m^{-2} (at 14 V), respectively. © 2007 Wiley Periodicals, Inc. J Polym Sci Part A: Polym Chem 45: 3243–3255, 2007
Keywords: 9,9-dipropylfluorene; 2,2′:6′,2″-terpyridyl unit; metallo-polymers; PLED; Sonogashira coupling reaction; zinc(II) ion

INTRODUCTION

Many different coordination polymers with bipyridyl or terpyridyl backbones have been investigated over last few decades while searching for new smart materials.[1–23] Especially, the interest regarding 2,2′:6′,2″-terpyridyl (tpy) units has increased, because tpy units have very high bonding affinities toward transition metal ions because of the chelating effect and $d\pi \rightarrow p\pi^*$ back bonding of metals to the pyridyl rings.[24] Upon addition of proper metal ions, metallo-polymers can be built from the bifunctional monomers containing bistpy moieties. The general concept of functionalized bistpy telechelics to give coordination metallo-polymers was presented in 1995.[13] It was proven that metallo-polymers generated by complexation of two tpy units with transition metal ions gave octahedral coordination geometries,[8] and possessed distinct photophysical, electrochemical, and magnetic properties.[25]

Using zinc(II) ions as templates to assemble organic building blocks into polymer chains through complexation of tpy units is an appealing strategy for the construction of photoluminescent (PL) or electroluminescent (EL) metallo-polymers with well-defined structures.[26–29] Lately,

Correspondence to: Prof. H.-C. Lin (E-mail: linhc@cc.nctu.edu.tw)

Journal of Polymer Science: Part A: Polymer Chemistry, Vol. 45, 3243–3255 (2007)

Dobrawa and Würthner reported that metallopolymers containing perylene bisimide dyes bearing (tpy)zinc(II) moieties showed high quantum yields and strong red emissions in PL.[30] According to Che and coworkers' report, the incorporations of (tpy)zinc(II) moieties into different main-chain structures exhibited different emission colors ranging from violet to yellow with high PL quantum yields and EL performance.[26] Moreover, the well-defined light-emitting metallo-*alt*-copolymer containing terpyridyl zinc(II) moieties has been reported by us recently.[26,31]

It is confirmed that the phenomenon of metal to ligand charge transfer (MLCT) does not occur in (tpy)zinc(II) complexes because of the d^{10} zinc(II) species, so only intraligand charge transfer (ILCT) happens between (tpy)zinc(II) coordination sites and chromophores even in fully conjugated metallo-polymers.[32,33] Therefore, the incorporation of (tpy)zinc(II) moieties into the metallo-polymers with fine-tuned chromophores can provide good quantum yields[26,30] and thermal stabilities,[26] and thus to have the potential to become high-performance emissive or host materials in PLED applications.

Herein, the syntheses of conjugated bistpy monomers containing identical chelating functions, which were linked to 9,9-dipropylfluorene units via phenylene/ethynylene fragments, and self-assembled processes of bistpy monomers with zinc(II) ions to afford (tpy)zinc(II) metallopolymers are presented. In addition, the PL, thermal, electrochemical, and EL properties will be reported as well.

EXPERIMENTAL

Measurements

^{1}H NMR spectra were recorded on a Varian unity 300 MHz spectrometer using $CDCl_3$ solvents. Elemental analyses were performed on a HERAEUS CHN-OS RAPID elemental analyzer. Transition temperatures were determined by differential scanning calorimetry (DSC) (PerkinElmer Pyris 7) at a heating and cooling rate of 10 °C min^{-1}. Thermogravimetric analysis (TGA) was conducted on a Du Pont Thermal Analyst 2100 system with a TGA 2950 thermogravimetric analyzer at a heating rate of 20 °C min^{-1} under nitrogen. Viscosity measurements were proceeded by comparing polymer solutions (10% weight ratio in NMP) with the corresponding monomer solutions in the same condition (with viscosity $\eta = 6$ cp) on a BROOKFILEL DV-III + RHEOMETER system at 25 °C (100 rpm, Spindle number: 4). UV-Visible (UV-Vis) titration experiments were preformed by that 1.0×10^{-5} M monomer solutions in the solvent of $CH_3CN/CHCl_3$ (2/8 in volume) were titrated with 50 μL aliquots of 3.9×10^{-4} M $Zn(OAc)_2$ solutions in the solvent with the same composition. UV-Vis absorption spectra were recorded in dilute DMF solutions (10^{-5} M) on a HP G1103A spectrophotometer, and fluorescence spectra were obtained on a Hitachi F-4500 spectrophotometer. Fluorescence quantum yields in solutions were determined relative to the integrated photoluminescence (PL) density of quinine sulfate in 1 N sulfuric acid with a known quantum yield (ca. 5×10^{-5} M, quantum yield = 0.55) in solutions. Cyclic voltammetry (CV) was performed at a scanning rate of 100 mV s^{-1} on a BAS 100 B/W electrochemical analyzer, which was equipped with a three-electrode cell. Pt wire was used as a counter electrode, and an Ag/AgCl electrode was used as a reference electrode in the CV measurements. The polymer thin films were cast onto a Pt disc as a working electrode with ferrocene as a standard in acetonitrile, and 0.1 M tetrabutylammonium hexafluorophosphate ($TBAPF_6$) was used as a supporting electrolyte. Polymer thin films were spin-coated on a quartz substrate from DMF solutions with a concentration of 10 mg mL^{-1}. A series of double-layer EL devices with the configuration of ITO/PEDOT:PPS/Polymer/LiF/Al were made. The solutions (10 mg mL^{-1}) of light-emitting materials in DMF were spin-coated on glass slides precoated with indium tin oxide (ITO) having sheet resistances of ~20 Ω/square and an effective device area of 3.14 mm^2. The ITO glasses were routinely cleaned by ultrasonic treatment in detergent solutions and diluted water, followed by through rinsing in acetone and then ethanol. After drying, the ITO glasses were kept in oxygen plasma for 4 min before being loaded into the vacuum chamber. The spin coating rate was 6000 rpm for 60 s with PEDOT:PPS, 3000 rpm for 60 s with polymers, and the thicknesses of polymers were about 47–70 nm. One thin layer of LiF (1 nm) was deposited thermally as a cathode at a rate of 0.1–0.2 Å s^{-1} under a pressure of $\sim 2 \times 10^{-5}$ torr in an Ulvac Cryogenic deposition system, which was capped with 150 nm of aluminum. The current-voltage-luminescence properties were measured in ambient conditions with a Keithley 2400

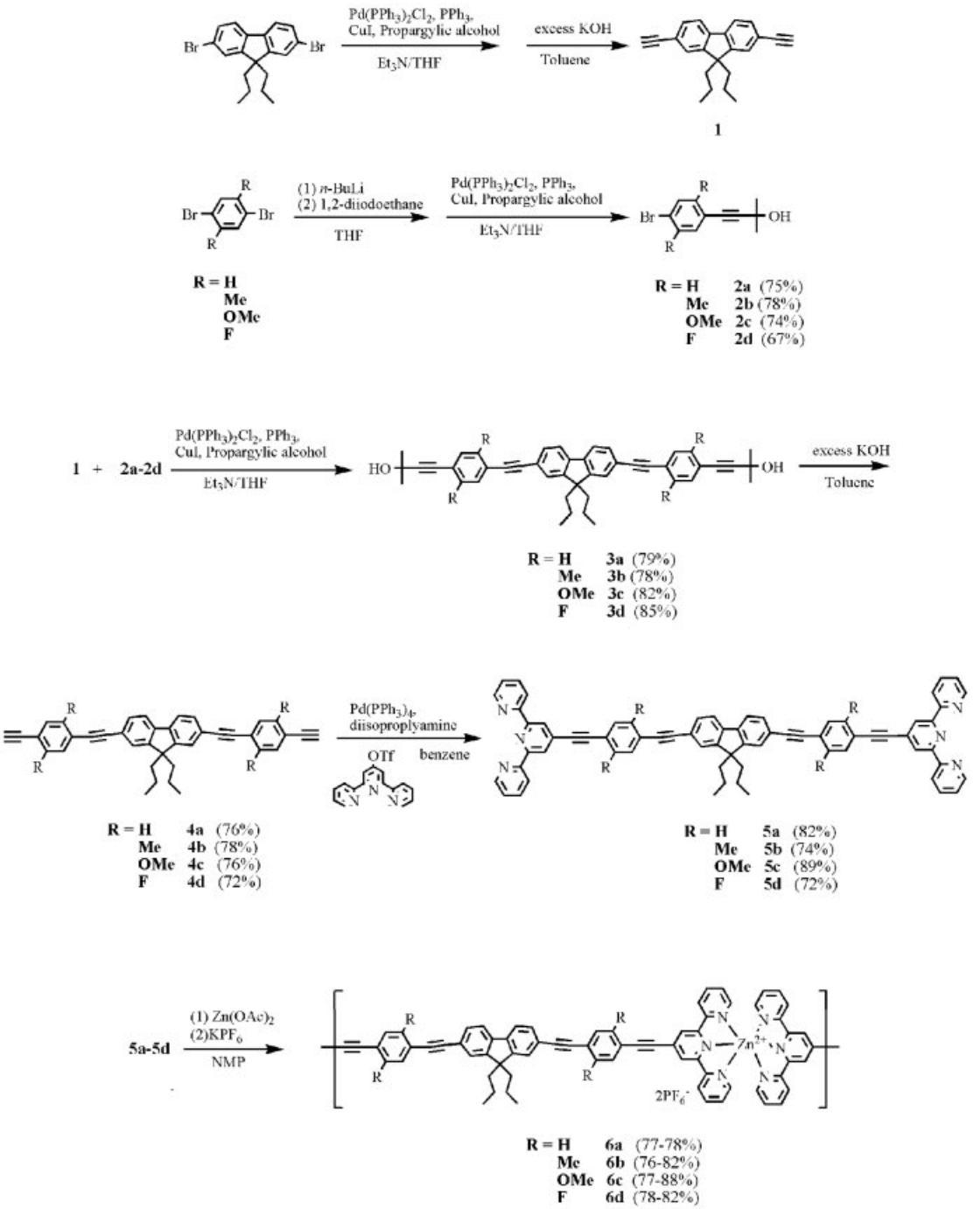

Scheme 1. Synthetic routes of monomers (**5a-5d**) and polymers (**6a-6d**).

Source meter and a Newport 1835C Optical meter equipped with an 818ST silicon photodiode.

Materials

Chemicals and solvents were reagent grades and purchased from Aldrich, ACROS, TCI, and Lancaster Chemical. Solvents were purified and dried according to standard procedures. Chromatography was performed with Merck silica gel (mesh 70–230) and basic alumina oxide, which was deactivated with 4 wt % of water. The synthetic routes of bis-2,2′:6′,2′-terpyridyl monomers (**5a-5d**) and metallo-polymers (**6a-6d**) are illustrated in Scheme 1.

Synthesis of Monomers

2,7-Diethynyl-9,9-dipropylfluorene (1)

Compound **1**[34] and starting materials **2a-2d**, that is 1,4-dibromo-2,5-dimethoxybenzene,[35] 1-bromo-4-iodo-2,5-disubstitutentbenzene,[36] and 4′[[(trifluoromethyl)sulfonyl]oxy]-2,2′:6′,6″-terpyridines,[37] were prepared and purified according to the literature procedures. Triethylamine and diisopropylamine were dried over suitable reagents and freshly distilled under nitrogen before using Schlenk tube techniques.[37]

1-Bromo-4(3-hydroxy-3-methylbutynyl) benzene (2a)

To a solution of 1-bromo-4-iodobenzene (8 g, 28 mmol) in 60 mL of THF/Et_3N (2/1), 3-methyl-1-butyn-3-ol (2.76 mL, 27 mmol) was added. After the solution was degassed with nitrogen for 30 min, $Pd(PPh_3)_2Cl_2$ (0.19 g, 0.28 mol), PPh_3 (2.9 g, 11 mol), and CuI (0.53 g, 2.8 mol) were added. The reaction was then refluxed at 70 °C under N_2 for 12 h. The solvent was removed under reduced pressure. The resulting solid was extracted with CH_2Cl_2/H_2O then dried over $MgSO_4$. The crude product was purified by column chromatography (silica gel, hexane/ethyl acetate = 4/1) to afford a white solid (4.65 g). ^{1}H NMR (300 MHz, $CDCl_3$): δ 7.44 (d, J = 7.5 Hz, 2H), 7.28 (d, J = 7.2 Hz, 2H), 2.03 (s, 1H), 1.61 (s, 6H). Yield: 75%. FABMS: m/e 238; $C_{11}H_{11}BrO$ requires m/e 238.10.

1-Bromo-2,5-dimethyl-4(3-hydroxy-3-methylbutynyl)benzene (2b)

The procedure is analogous to that described for (**2a**).Yield: 78%. ^{1}H NMR (300 MHz, $CDCl_3$): δ 7.37 (s, 1H), 7.24 (s, 1H), 2.49 (s, 3H), 2.38 (s, 3H), 2.04 (s, 1H), 1.63 (s, 6H). FABMS: m/e 266; $C_{13}H_{15}BrO$ requires m/e 266.15.

1-Bromo-2,5-dimethoxyl-4(3-hydroxy-3-methylbutynyl)benzene (2c)

The procedure is analogous to that described for (**2a**). Yield: 74%. ^{1}H NMR (300 MHz, $CDCl_3$): δ 7.06 (s, 1H), 6.91 (s, 1H), 3.84 (s, 3H), 3.82 (s, 3H), 2.67 (s, 1H), 1.64 (s, 6H). FABMS: m/e 298; $C_{13}H_{15}BrO_3$ requires m/e 298.15.

1-Bromo-2,5-difluoro -4(3-hydroxy-3-methylbutynyl)benzene (2d)

The procedure is analogous to that described for (**2a**). Yield: 67%. ^{1}H NMR (300 MHz, $CDCl_3$): δ 7.27 (dd, J_1 = 5.7 Hz, J_2 = 5.7 Hz, 1H), 7.13 (dd, J_1 = 6 Hz, J_2 = 6 Hz, 1H), 2.10 (s, 1H), 1.60 (s, 6H). FABMS: m/e 274; $C_{11}H_9BrF_2O$ requires m/e 273.98.

2,7-Bis[(3-hydroxy-3-methylbutynyl)-phenylethynyl]-9,9-dipropylfluorene (3a)

A mixture of 2,7-diethynyl-9,9-dipropylfluorene (0.71 g, 2.38 mmol) and (**2a**) (1.31 g, 5.9 mmol) was dissolved in 60 mL of Et_3N/THF. After the solution was degassed with N_2 for 30 min, $Pd(PPh_3)_2Cl_2$ (20 mg, 0.024 mol), PPh_3 (250 g, 0.95 mmol), and CuI (47 mg, 0.24 mmol) were added with mechanical stirring. The reaction was then refluxed at 80 °C under N_2 over 24 h. The solvent was removed under reduced pressure. The resulting solid was extracted with CH_2Cl_2/H_2O then dried over $MgSO_4$. The crude product was purified by column chromatography (silica gel, hexane/dichloromethane = 4/1) to afford a yellow solid (1.1 g). ^{1}H NMR (300 MHz, $CDCl_3$): δ 7.70 (d, J = 8.1 Hz, 2H), 7.51–7.56 (m, 8H), 7.42–7.45 (m, 4H), 2.05 (s, 2H), 1.99 (br, 4H), 1.65 (s, 12H), 0.69 (br, 10H). Yield: 79%. FABMS: m/e 615; $C_{45}H_{42}O_2$ requires m/e 614.81.

2,7-Bis[(3-hydroxy-3-methylbutynyl)-2,5-dimethy-phenylethynyl]-9,9-dipropyl fluorene (3b)

The procedure is analogous to that described for (**3a**). ^{1}H NMR (300 MHz, $CDCl_3$): δ 7.66 (d, J = 7.8 Hz, 2H), 7.52–7.48 (m, 4H), 7.37 (s, 2H), 7.28 (s, 2H), 2.49 (s, 6H), 2.38 (s, 6H), 2.03 (s, 2H), 1.98 (br, 4H), 1.65 (s, 12H), 0.69 (br, 10H). Yield: 78%. FABMS: m/e 671; $C_{49}H_{50}O_2$ requires m/e 670.92.

2,7-Bis[(3-hydroxy-3-methylbutynyl)-2,5-dimethoxy-phenylethynyl]-9,9-dipropyl fluorene (3c)

The procedure is analogous to that described for (**3a**). ^{1}H NMR (300 MHz, $CDCl_3$): δ 7.66 (d, J = 8.4 Hz, 2H), 7.56–7.54 (m, 4H), 7.04 (s, 2H), 6.94 (s, 2H), 3.92 (s, 6H), 3.87 (s, 6H), 2.13 (s, 2H), 1.96 (br, 4H), 1.66 (s, 12H), 0.69 (br, 10H). Yield: 82%. FABMS: m/e 735; $C_{49}H_{50}O_6$ requires m/e 734.92.

2,7-Bis[(3-hydroxy-3-methylbutynyl)-2,5-difluoro-phenylethynyl]-9,9-dipropyl fluorene (3d)

The procedure is analogous to that described for (**3a**). ^{1}H NMR (300 MHz, $CDCl_3$): δ 7.69 (d, J = 8.1 Hz, 2H), 7.56–7.53 (m, 4H), 7.24 (dd, J_1 = 8.7, J_2 = 6 Hz, 2H), 7.16 (dd, J_1 = 8.7, J_2 = 6 Hz, 2H), 2.09 (s, 2H), 1.98 (br, 4H), 1.64 (s, 12H), 0.68 (br, 10H). Yield: 75%. FABMS: m/e 687; $C_{45}H_{38}F_4O_2$ requires m/e 686.78.

2,7-Bis(phenylethynyl)-9,9-dipropylfluorene (4a)

A mixture of (**3a**) (1 g, 1.63 mmol) and KOH (365 mg, 6.5 mmol) in 60 mL of toluene was refluxed under N_2 with a vigorous stirring for 3 h. The solvent was then removed and crude product was purified by column chromatography (silica gel, hexane) to afford a white solid (6.1g). ^{1}H NMR (300 MHz, $CDCl_3$): δ 7.69 (d, J = 8.1 Hz, 2H), 7.56–7.49 (m, 12H), 3.20 (s, 2H), 1.99 (br, 4H), 0.69 (br, 10H). Yield: 76%. FABMS: m/e 499; $C_{39}H_{30}$ requires m/e 498.66.

2,7-Bis(2,5-dimethy-phenylethynyl)-9,9-dipropylfluorene (4b)

The procedure is analogous to that described for (**4a**). ^{1}H NMR (300 MHz, $CDCl_3$): δ 7.67 (d, J = 7.8.Hz, 2H), 7.53–7.49 (m, 4H), 7.39 (s, 2H), 7.35 (s, 2H), 3.34(s, 2H), 2.49 (s, 6H), 2.42 (s, 6H), 1.98 (br, 4H), 0.69 (br, 10H). Yield: 78%. FABMS: m/e 555; $C_{43}H_{38}$ requires m/e 554.76.

2,7-Bis(2,5-dimethoxy-phenylethynyl)-9,9-dipropylfluorene (4c)

The procedure is analogous to that described for (**4a**). ^{1}H NMR (300 MHz, $CDCl_3$): δ 7.67 (d, J = 8.4 Hz, 2H), 7.57–7.53 (m, 4H), 7.07 (s, 2H), 7.02 (s, 2H), 3.92 (s, 12H), 3.42 (s, 2H), 1.97 (br, 4H), 0.67 (br, 10H). Yield: 76%. FABMS: m/e 619; $C_{43}H_{38}O_4$ requires m/e 618.76.

2,7-bis(2,5-difluoro-phenylethynyl)-9,9-dipropylfluorene (4d)

The procedure is analogous to that described for (**4a**). ^{1}H NMR (300 MHz, $CDCl_3$): δ 7.79 (d, J = 87.5 Hz, 2H), 7.56–7.53 (m, 4H), 7.19–7.27 (m, 4H), 3.42 (s, 2H), 2.01 (br, 4H), 0.67 (br, 10H). Yield: 72%. FABMS: m/e 571; $C_{39}H_{26}F_4$ requires m/e 570.62.

Monomer 5a

Compound **4a** (250 mg, 0.5 mmol) and 4′-[[(trifluoromethyl)sulfonyl]oxy]-2,2′:6′,6″-terpyridine (420 g, 1.1 mmol) were dissolved in nitrogen-degassed benzene, then [$Pd^0(PPh_3)_4$] (70 mg, 0.06 mmol) was added and followed by nitrogen-degassed $^iPr_2NH$. The solution was then heated to 70 °C. After complete consumption of starting materials, the solvent was evaporated and the product was purified by column chromatography (alumina, hexane/dichloromethane = 10/1) to afford a yellow solid (393 mg). ^{1}H NMR (300 MHz, $CDCl_3$): δ 8.73 (d, J = 5.4 Hz, 4H), 8.59–8.65 (m, 8H), 7.89 (t, J = 7.2 Hz, 4H), 7.69 (d, J = 7.5 Hz, 2H), 7.56–7.58 (m, 12H), 7.35–7.38 (m, 4H), 2.00 (br, 4H), 0.70 (br, 10H). Yield: 82%. FABMS: m/e 961; $C_{69}H_{48}N_6$ requires m/e 960.39. Anal. Calcd for $C_{69}H_{48}N_6$: C, 86.22; H, 5.03; N, 8.74. Found: C, 85.89; H, 4.99; N, 8.30.

Monomer 5b. *The procedure is analogous to that described for monomer* 5a

^{1}H NMR (300 MHz, $CDCl_3$): δ 8.76 (d, J = 5.4 Hz, 4H), 8.58–8.67 (m, 8H), 7.91 (t, J = 8.1 Hz, 4H), 7.69 (d, J = 7.8 Hz, 2H), 7.53–7.56 (m, 4H), 7.45 (s, 4H), 7.37–7.41 (m, 4H), 2.55 (s, 12H), 2.01 (br, 4H), 0.71 (br, 10H). Yield: 74%. FABMS: m/e 1018; $C_{73}H_{56}N_6$ requires m/e 1017.27. Anal. Calcd for $C_{73}H_{56}N_6$: C, 86.19; H, 5.55; N, 8.26. Found: C, 85.77; H, 5.12; N, 8.12.

Monomer 5c. *The procedure is analogous to that described for monomer* 5a

^{1}H NMR (300 MHz, $CDCl_3$): δ 8.73 (d, J = 5.4 Hz, 4H), 8.62–8.65 (m, 8H), 7.88 (t, J = 7.5 Hz, 4H), 7.69 (d, J = 8.4 Hz, 2H), 7.56–7.59 (m, 4H), 7.34–7.38 (m, 4H), 7.10 (s, 4H), 3.97(s, 6H), 3.96 (s, 6H), 1.99 (br, 4H), 0.69 (br, 10H). Yield: 89%. FABMS: m/e 1082; $C_{73}H_{56}N_6O_4$ requires m/e 1081.26. Anal. Calcd for $C_{73}H_{56}N_6O_4$: C, 81.09; H, 5.22; N, 7.77. Found: C, 81.34; H, 5.23; N, 7.56.

Monomer 5d. *The procedure is analogous to that described for monomer* 5a

^{1}H NMR (300 MHz, $CDCl_3$): δ 8.73 (d, J = 4.8 Hz, 4H), 8.61–8.64 (m, 8H), 7.88 (t, J = 7.2 Hz, 4H), 7.69 (d, J = 7.8 Hz, 2H), 7.56–7.59 (m, 4H), 7.35–7.39 (m, 4H), 7.27–7.33 (m, 4H), 2.01 (br, 4H), 0.71 (br, 10H). Yield: 72%. FABMS: m/e 1034;

$C_{69}H_{44}F_4N_6$ requires m/e 1033.12. Anal. Calcd for $C_{69}H_{44}F_4N_6$: C, 80.22; H, 4.29; N, 8.13. Found: C, 79.80; H, 4.16; N, 8.34.

Polymer 6a

To monomer **5a** (500 mg, 0.52 mmol) in 30 mL of *N*-methylpyrrolidinone (NMP) solution, zinc acetate (114.16 mg, 0.52 mmol) in NMP (10 mL), was added dropwise. The resulting solution was heated at 105 °C under a nitrogen atmosphere. After stirring for 24 h, excess KPF_6 was added into the hot solution. The resulting solution was poured into methanol and the precipitate obtained was purified by washing with acetone. The polymers were dried under vacuum at 40 °C for 24 h and collected as yellow solids. Yields: 77–82%.

Polymers 6b-6d

The procedure Is analogous to That described for polymer **6a**. Yields: 76–88%.

RESULTS AND DISCUSSION

Synthesis and Characterization

The synthetic routes of the monomers (**5a-5d**) and metallo-polymers (**6a-6d**) are demonstrated in Scheme 1. Compound **1** was synthesized by the reaction of 2,7-dibromo-9,9-dipropylfluorene with propargylic alcohol via the Sonogashira coupling reaction, and further deprotection by refluxing toluene in a basic condition. To obtain a series of compounds **2a-2d** in good yields, it is necessary to convert bromine substitutents into iodine substitutents by metal-halogen exchange before proceeding the Pd catalyzed alkyne-aryl-coupling reaction selectively. Various combinations of compounds **3a-3d** allow the conjunction of compound **1** with compounds **2a-2d** in similar coupling reactions followed by deprotection under a basic condition, which led to compounds **4a-4d** bearing acetylene groups. To access a family of monomers, the monomer ligands **5a-5d** were prepared in 75% overall yields by cross-coupling reactions between **4a-4d** and 4′-[[(trifluoromethyl)sulfonyl]-oxy]-2,2′:6′,2″-terpyridine (tpy-OTf) in the presence of catalytic amounts of Pd(0) complexes under a basic condition.[38] In fact, monomers **5a-5d** were readily prepared by Pd(0)-promoted reactions using appropriate solvents (benzene and toluene) and reaction time, which could produce the required products in excellent yields. Finally, meatllo-polymers **6a-6d** were synthesized by refluxing with zinc acetate in NMP solutions and followed by subsequent anion exchange. Yields of all polymers were up to 77–88% after repeated washing with acetone. In contrast to other polymerization methods, such as the Wittig or Heck coupling reaction, the present procedure does not need any catalyst.[39,40] The reactivity of zinc(II) ions and the stability of six-coordinate bis(tpy)zinc(II) moieties allow the self-assembled reaction to take place under mild conditions.

All pure monomers (**5a-5d**) are soluble in most chlorinated solvents and isolated as yellow powders, which were also characterized by ^{1}H NMR, mass spectrometry, UV-Vis spectrometry, and elemental analysis. Compared with the monomers, the metallo-polymers (**6a-6d**) have less solubility because of the rigid linear cores of the polymers, which depends on the lateral sizes of substitutents attached to the phenylene rings, that is solubility: OMe (**6c**) > Me (**6b**) > F (**6d**) > H (**6a**). Moreover, these polymers are only soluble in some polar solvents, for instance DMSO, DMAc, and DMF.

^{1}H NMR Titration

To confirm the formation of these metallo-polymers, ^{1}H NMR titration is an important tool for the analysis of self-assembled processes where the stoichiometries of the metal ions and monomer ligands need to be carefully controlled in a ratio of 1:1. The studies of ^{1}H NMR titration in Figure 1 were carried out by varying the molar ratios of zinc(II) ions to monomer **5c** in deuterated dimethylsulfoxide (DMSO-d_6). The addition of zinc(II) ions to monomer **5c** resulted in a number of dramatic shifts in ^{1}H signals around the aromatic regions. The ^{1}H signals of free monomer **5c** around 8.8–8.0 and 7.6 ppm belonged to tpy rings, and those (two peaks) around 7.4 ppm belong to *p*-dimethoxyphenylene rings. It is worthy noting that the ^{1}H signals of fluorene units are around 7.95 and 7.7 ppm. As the molar ratio of **5c**/Zn^{2+} = 1/0.2, these ^{1}H signals started to change and new signals around 8.9, 8.3, and 7.8 ppm became noted. When the ratio of **5c**/Zn^{2+} reaches 1/0.7, all conceivable signals belonging to tpy rings in free monomer **5c** were not observed, and the signals (two peaks around 7.4 ppm) of *p*-dimethoxyphenylene rings also merged into a

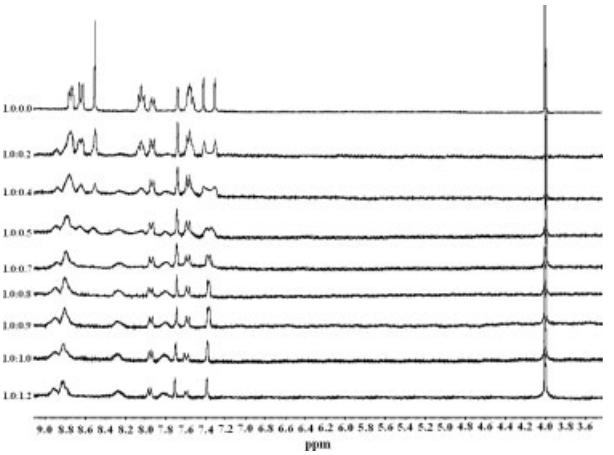

Figure 1. ^{1}H NMR spectra with different ratios (**5c**:Zn^{2+}) of monomer (**5c**) to metal ions (Zn^{2+}) in DMSO (5 mM) from free **5c** (top, **5c**:Zn^{2+} = 1:0) to polymer **6c** (next to bottom, **5c**:Zn^{2+} = 1:1).

single peak (except for that of the central fluorene rings). These phenomena originated from the electron delocalization happened between zinc(II)-tpy units and central chromophore (fluorenyl/ethynylene/phenylene) components which induced new ^{1}H signals in terpyridyl units and the signals (two peaks around 7.4 ppm) of *p*-dimethoxyphenylene were broaden and merged into a single peak. Furthermore, the conjugated distance between the tpy rings and the central fluorene rings (separated by a phenylene unit and two ethynylene bridges) that are long enough to avoid the influence of the coordination processes. Until the ratio of **5c**/Zn^{2+} reached 1/1, all variations in ^{1}H signals became saturated, and the solution remained clear and no precipitation or further aggregation was observed. Even after increasing the ratio of **5c**/Zn^{2+} up to 1/1.2, no further shifts and changes of ^{1}H signals were detected in the ^{1}H NMR spectrum. Therefore, the alteration of ^{1}H signals during NMR titration was attributed to the coordination process among the metal ions and tpy units.[30] On the basis of these data, the formation of all coordination polymers (**6a-6d**) containing monomers (**5a-5d**) can be concluded. Dobrawa, Würthner, and Che showed that the polymer formation can be controlled by the exact stoichiometric ratios of the metal ions to the monomer ligands.[26,30,31] Exceeding the stoichiometric ratio of **5c**/Zn^{2+} over 1/1.2, the tpy units and zinc(II) ions will be in an over-coordinated situation to cause incomplete polymer chains, which will not be further discussed in this study.

UV-Visible Titration

To further characterize metallo-polymers **6a-6d**, they were also confirmed by UV-Vis titration experiments. Upon addition of Zn^{2+} to monomer **5c** reaching a ratio of 1:1 (Zn^{+2}:**5c**) as shown in Figure 2, the spectra revealed a shift of three other absorption bands at 284, 317, 343, and 405 nm along with one isosbestic point, which suggests that an equilibrium occurred between a finite number of spectroscopically distinct species. The titration curves (Fig. 2, insets) showed a linear increase and a sharp end point at the ratio of 1:1 (Zn^{+2}:**5c**), indicating the formation of metallo-polymers. Furthermore, polymer **6c** displayed a shoulder in the lowest energy absorption at λ_{Abs} = 450 nm, which corresponded to a charge transfer occurring within the monomers between the electron rich central chromophore (fluorenyl/ethynylene/phenylene) components and the metal-coordinated (electron-deficient) terpyridyl moieties.[41]

Thermal Properties

The thermal properties of the monomers (**5a-5d**) and polymers (**6a-6d**) were studied by TGA and DSC, as summarized in Table 1. The decomposition temperatures (T_d) (5% weight loss measured by TGA) of the monomers under a nitrogen atmosphere ranged from 297 to 351 °C, and those of polymers ranged from 325 to 410 °C. The glass

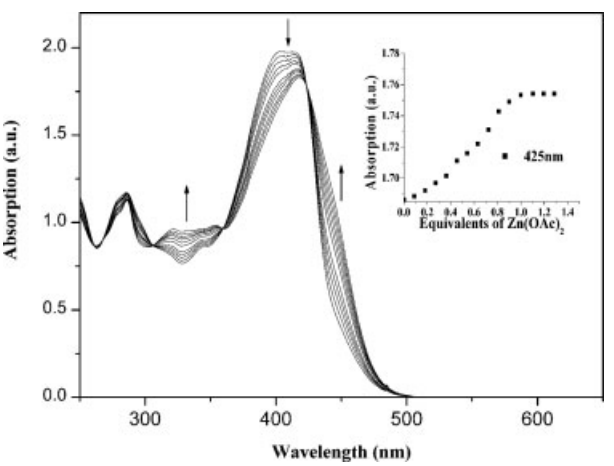

Figure 2. UV-Vis spectra acquired upon the titration of monomer **5c** in $CH_3CN/CHCl_3$ (2/8 in vol.) with $Zn(OAc)_2$. The spectra are shown at selected Zn^{+2}: **5c** ratios ranging from 0 to 1. The inset shows the normalized absorption at 425 nm as a function of Zn^{+2}: **5c** ratio.

Table 1. Thermal Properties of Monomers (**5a-5d**) and Polymers (**6a-6d**)

Compound	T_d[a] (°C)	T_m/T_c[b] (°C)	T_g[b] (°C)
5a	297	232/–	145
5b	311	254/–	149
5c	320	276/–	157
5d	351	294/145	197
6a	325	–[c]	–[c]
6b	342	–[c]	–[c]
6c	375	–[c]	–[c]
6d	410	–[c]	–[c]

[a] T_d was determined by TGA with heating rates of 20 °C min^{-1} under N_2 atmosphere.
[b] T_m (melting temperature), T_c (crystallization temperature), and T_g (glass transition temperature) were determined by DCS with heating/cooling rates of 10 °C under N_2 atmosphere.
[c] The transition temperatures of T_m, T_c, and T_g in polymers were not found in DSC scans.

transition temperatures of the monomers were characterized by DSC. For instance, monomer **5c** obviously possesses T_g (~157 °C) during the first cooling and second heating cycles. All monomers show high glass transition temperatures (T_g > 145 °C), which were affected by different lateral substituents (with different polarities and sizes) attached to the central conjugated structures. According to the glass transition temperatures of the monomers: **5d** (F) > **5c** (OMe) > **5b** (Me) > **5a** (H), it seems that the polarity effect (of the lateral substituents) is more influential than the size effect (of the lateral substituents) on the T_g values of the monomers. In addition, similar trends (i.e. the dipole moment effects of the lateral substituents) also occurred in the melting temperatures (T_m) and the decomposition temperatures (T_d) for both monomers and polymers, that is **5**d > **5c** > **5b** > **5a** and **6d** > **6c** > **6b** > **6a**. In general, the result of high T_g values in monomers can be attributed to the rigid and linear conformation of monomers.

In comparison with monomers, the increases of the decomposition temperatures (T_d) of metallo-polymers **6a-6d** in Table 1 were observed and similar results in coordination polymers were reported in the literature.[22,37] Owing to the coordination, it was found that 25–30 wt % of the residual materials were left upon heating polymers to 800 °C. Similar to another report,[42] no phase transitions were observed in the DSC measurements of polymers **6a-6d**. However, as described in the elevation of decomposition temperatures (T_d) of polymers in contrast to monomers, the glass transition temperatures (T_g) of coordination polymers should be higher than those of monomeric counterparts.

Viscosity and Electrochemical Properties

The viscosity and electrochemical properties of the polymers (**6a-6d**) were studied by rheometer and CV, as summarized in Table 2. By adding Zn^{2+} ions into monomer solutions, the formation of metallo-polymers **6a-6d** was confirmed by the enhancement of the viscosities (up to 1.5–1.83 times) relative to those of their analogous monomers. Similar results have also been reported by Gordaninejad's group.[43]

To determine the energy band structures of PLED materials, it is necessary to measure the energy levels of the highest occupied molecular orbital (HOMO) and the lowest unoccupied molecular orbital (LUMO) of all light-emitting metallo-polymers **6a-6d**, which were carried out by CV to investigate the oxidox/redox behavior of the polymer thin films and their electrochemical properties are summarized in Table 2.

Table 2. Electrochemical and Viscosity Properties of Polymers (**6a-6d**)

Polymer	η[a] (cp)	$E_{1/2}$ (red)[b] (V)	E_{onset} (red) (V)	LUMO[c] (eV)	Band Gap[d] (eV)
6a	9	−1.12(r), −2.13, −2.51, −2.64	−0.98	−3.32	3.00
6b	10	−1.13(r), −2.18, −2.57, −2.72	−0.95	−3.35	2.88
6c	11	−1.14(r), −2.26, −2.61, −2.82	−0.89	−3.41	2.78
6d	10	−1.18(r), −2.13, −2.39, −2.64	−0.99	−3.31	2.95

[a] Monomers **5a-5d** dissolved in NMP (by 10% weight ratio with viscosity η = 6 cp at 25 °C) were used as a reference to determine the viscosities of the polymers.
[b] Half-wave potential in N_2-purged acetonitrile, r in parentheses indicates a reversible process.
[c] LUMO level was calculated from the measured reduction potential versus ferrocene/ferrocenium couple in acetonitrile.
[d] The optical band gaps were estimated from the absorption spectra in solid films by extrapolating the tails of the lower energy peaks.

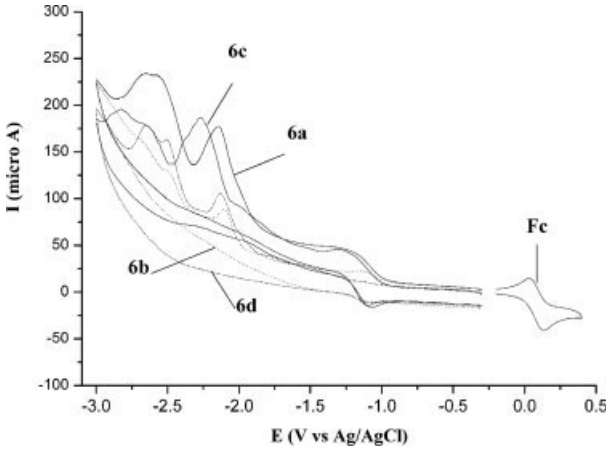

Figure 3. Cyclic voltammetry (CV) measurements of polymers **6a**-**6d** during the reduction processes.

All metallo-polymers (**6a-6d**) exhibit quasi-reversible reduction wave at $E_{1/2}$ value of −1.12 to −1.18 V in cathodic scans up to −3 V. The reduction curves of polymers **6a-6c** (in Fig. 3) were attributed to the reduction of tpy units in metal complexes.[29] Other reduction processes take place at more negative potentials, but they are not well defined. The absence of oxidation process in these polymers was expected, because metal oxidation is extremely difficult to be observed for the d^{10} zinc(II) ion species (the anodic sacns up to 1 V).[26,44] The LUMO levels estimated here are based on the reference energy level of ferrocene (4.8 eV below the vacuum level) according to the following equation[45]: $E^{\mathrm{LUMO}} = [\ -(E^{\mathrm{onset}} - 0.50) - 4.8]$ eV. The optical band gaps were estimated from absorption spectra in solid films by extrapolating the tails of the lowest energy peaks. Moreover, the band gaps of polymers **6a** (3.0 eV) and **6d** (2.95 eV) were quite similar, and their films both showed green PL. Polymer **6c** had the smallest band gap (2.78 eV) and gave a yellow emission.[21,26]

Photophyscial Properties

To further investigate the photophyscial properties, the UV-Vis absorption and PL spectra of the monomers (**5a-5d**) and polymers (**6a-6d**) in both solutions (DMF as solvent) and solid films were measured and summarized in Table 3. It is noted that similar absorption patterns between 270 and 500 nm were observed in these monomers and polymers with various lateral substitutions. In general, three major absorption peaks were observed in the absorption spectra for all compounds (in solutions and solid films), where the shorter absorption peaks around 283–342 nm belong to the tpy units and the central fluorene/phenylene cores, and the longest absorption peak belongs to their charge-transfer (CT) transition states. For the longest absorption peaks, the values of $\lambda_{\max}$ have the order of **c** (OMe) > **b** (Me) > **a** (H) because the electron-donating (ED) effect, with the exception of **6d** (F) on account of the electron-withdrawing (EW) effect. When strong ED (OMe) group was laterally attached to the conjugated core, the CT transition state was progressively shifted toward lower energy. However, monomer **5d** (with lateral F units) did not

Table 3. Photophyscial Properties of Monomers (**5a-5d**) and Polymers (**6a-6d**)

Compound	$\lambda_{\mathrm{max,Abs.,sol}}$[a,b] (nm)	$\lambda_{\mathrm{max,PL,sol}}$/$\Phi_{\mathrm{PL,sol}}$[a,b,c] (nm)	$\lambda_{\mathrm{max,Abs.,film}}$[d] (nm)	$\lambda_{\mathrm{max,PL,film}}$/$\Phi_{\mathrm{PL,film}}$[d,e] (nm)
5a	285,319,375	417(432)/0.27	286,318,374	495/–[f]
5b	284,321,381	421(436)/0.18	285,322,380	507/–[f]
5c	285,342,402(415)	440(460)/0.29	286,343,404	530/–[f]
5d	284,322,382	444/0.21	285,321,383	494/–[f]
6a	283,316,362	435/0.38	284,316,364	545/0.35
6b	283,321,371	421(438)/0.31	283,322,372	559/0.26
6c	284,340,397	440(461)/0.41	283,341,396	570/0.37
6d	283,320,370	449/0.33	283,318,369	528/0.32

[a] Concentration of 1×10^{-5} M in DMF.
[b] The absorption and PL emission shoulders are shown in the parentheses.
[c] Quinine sulfate in 0.1 N of sulfuric acid used as a reference to determine the quantum yields (Φ_{PL}) of PL in solutions.
[d] The thicknesses of films are around 47–70 nm.
[e] 9,10-diphenylanthracene doped in PMMA was used as a reference to determine the quantum yields (Φ_{PL}) of PL in solid films.
[f] The quantum yields (Φ_{PL}) of PL in solid films are too small to be detected in monomers **5a-5d**.

exhibit an obvious blue shift of absorption (λ_{max} = 382 nm in solutions, as shown in Table 3) in the CT transition state, that could be attributed to a weak EW effect. In addition, all polymers showed no significant changes in the absorption transition bands.

All monomers and polymers exhibit intensive violet to blue PL emissions (λ_{max} = 417–449 nm) in DMF solutions (shown in Table 3). The aggregation effect of monomers (**5a-5d**) and polymers (**6a-6d**) can be compared by the PL spectra in the solid states from Table 3. In contrast to $\lambda_{max,PL}$ values in solutions, polymers have Stokes shifts (red shifts) of $\lambda_{max,PL}$ values (ca. red shifts of 130 nm) in solid films than analogous monomers (ca. red shifts of 80 nm), except for monomer **5d** and polymer **6d**. This suggests that the metallo-supramolecular structures of polymers have stronger aggregation than the monomers in solid films. However, smaller red shifts of $\lambda_{max,PL}$ values in lateral F substituted monomer **5d** and polymer **6d**, for instance a redshift of 50 nm in monomer **5d** and a redshift of 79 nm in polymer **6d**, which caused the shortest emission wavelength of PL in the solid films of monomer **5d** and polymer **6d** compared with their analogues in solutions, respectively. Importantly, the quantum yields of the coordination polymers (in both solutions and solid films) are higher than those of their analogous monomer ligands. Therefore, the particular metal ions, that is zinc(II), of these coordination polymers serving to increase electron delocalization on the polymer backbones induce the enhancement and red shifts of PL emissions in solid films.

In Figure 4, monomers **5a-5c** show a shoulder in their PL spectra (in solutions), except monomer **5d**. Whereas, monomer **5d** exhibits only one emission band and its full width at half-maximum (fwhm) value is broader than the others. The observed behavior is consistent with the difference of ED and EW effect in influencing the energy and transition dipole of the potential CT transitions localized on the monomers. Comparing the structures of monomers **5a**-**5c**, the sizes of their lateral subutitutents are in the order of **5c** (OMe) > **5b** (Me) > **5a** (H), so the intensities of their shoulders follow the order of **5c** < **5b** < **5a**. Furthermore, monomer **5c** and polymer **6c** (OMe) in solutions exhibited the smallest fwhm values in the PL emission spectra (Figs. 4 and 5). This indicates that the excimer emissions in PL solutions might be reduced by increasing the size of lateral substituents, so the phenomenon of excimer emission (in solutions) was minimized by increasing the steric hindrance, for example, monomer **5c** and polymer **6c**. However, this is not true for the solid film of polymer **6c** in Figure 5, because a strong aggregation effect (i.e. a large red-shifted $\lambda_{max,PL}$ value of 130 nm obtained by changing from the solution state to the solid state) still occurred in the solid state of polymer **6c**, which is also confirmed by the increase of the fwhm values in PL emissions of polymer **6c** in solid films (Fig. 5) compared with that of polymer **6c** in solutions (Figs. 4 and 5). Thus, the polymers (**6a-6d**) emitted green to yellow fluorescence (λ_{max} = 528–570 nm) in solid films, and these PL emissions showed large Stokes shifts, which were also attributed to excimer formation or aggregation in the solid films.[27,41] Here, we can find that even polymer **6c** possesses more

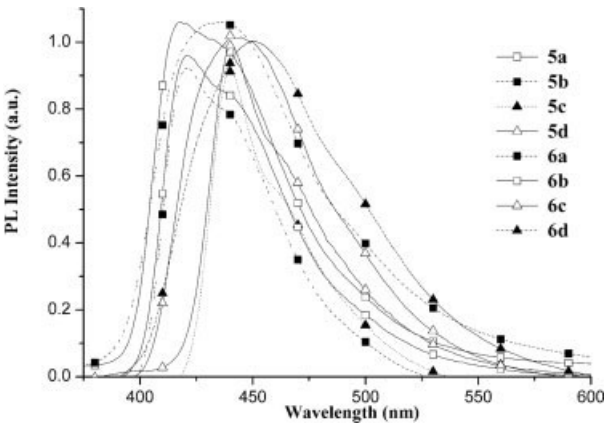

Figure 4. Normalized PL spectra of monomers (**5a-5d**) and polymers (**6a-6d**) in DMF solutions.

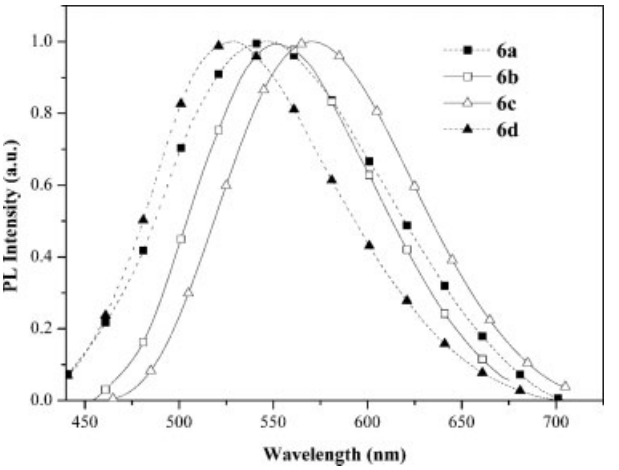

Figure 5. Normalized PL spectra of polymers (**6a-6d**) in solid films.

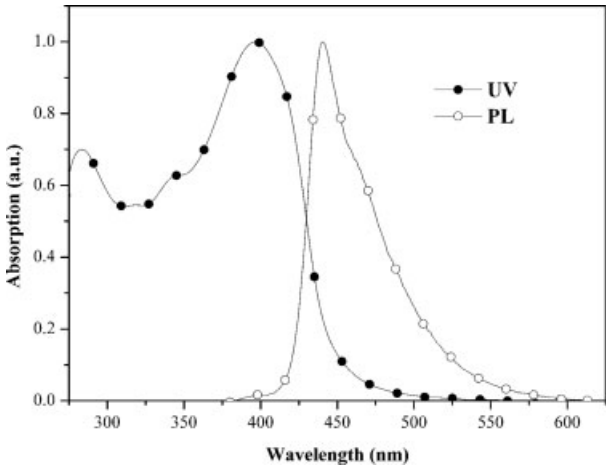

Figure 6. Normalized UV-Vis and PL spectra of polymer **6c** in DMF solutions.

bulky lateral substitutents (OMe) in the phenelyene rings; whereas, there is no significant influence on reduced aggregation of the polymer chains and suppression of the excimer formation in polymer **6c**. As a result, the lateral substitutents of -OMe in the phenylene rings are not bulky enough to have substantial effects on the reduction of aggregation from rigid conjugated cores in the polymers. Interestingly, the PL spectra of these monomers and polymers show poor mirror symmetry with the lowest energy absorption transition, and in fact, the UV-Vis and PL spectra are quite different from each other (in shape). For example, Figure 6 shows the UV-Vis and PL spectra of polymer **6c** (in solutions).[28]

Most importantly, the metallo-polymers exhibit higher PL quantum yields than the corresponding monomers (as shown in Table 3, i.e. $\Phi_{f,\mathrm{sol}} = 0.18$–$0.29$ for monomers in DMF and $\Phi_{f,\mathrm{sol}} = 0.31$–$0.41$ for polymers in DMF; $\Phi_{f,\mathrm{film}} = 0$ for monomer films and $\Phi_{f,\mathrm{film}} = 0.26$–$0.37$ for polymer films). Because of the poor film quality of monomers, the quantum yields of the monomers in solid films were not measured in the PL experiments. Therefore, luminescent bistpy units upon coordination to zinc(II) ions (possibly serving to increase electron delocalization on the polymer backbones) induce the enhancements and red shifts of PL emissions in solid films, which were also reported in recent publications.[26]

Electroluminescence Properties

The CV results show that both HOMO and LUMO energy levels of the metallo-polymers do not match the work functions of indium-tin oxide (ITO) anode and Al cathode. Therefore, we choose PEDOT and LiF/Al as the hole transporting layer and cathode, respectively, to overcome these large energy barriers. The electroluminescence (EL) properties of these polymers were investigated, except polymer **6a** due to its poor solubility. The other polymers (**6b-6d**) were used as emitting layers in a double-layer light-emitting devices with configuration of ITO/PEDOT:PSS/Polymer/LiF/Al. The function of LiF/Al as a cathode is because that the electron injection capability from a high work-function cathode can be significantly improved by inserting polar or ionic species between a metal electrode and a light-emitting layer.[46] The EL properties of PLED devices (device structure: ITO/PEDOT:PPS/Polymer(**6b-6d**)/LiF/Al) with good external quantum yields between 0.36 and 1.02 and maximum brightnesses between 323 and 931 cd m^{-2} (at 14 V) are listed in Table 4.

The emission colors of these devices (at a bias voltage around 10 V) were yellow to orange in Commission Internationale de l'Eclairage (CIE)

Table 4. Electroluminescence (EL) Properties of PLED Devices[a] Containing an Emitting Layer of Polymers (**6b-6c**)

Polymer	$\lambda_{\mathrm{max,EL}}$ (nm)	V_{on} (V)[b]	Max. Brightness (cd/m^2)	$\Phi_{\mathrm{EL}\ (\%)}$[c]	Power Efficiency (cd/A)	CIE Coordinates (x and y)
6b	558	5.8	323	0.36	0.13	(0.35, 0.41)
6c	598	5.5	931	1.02	0.33	(0.48, 0.45)
6d	553	6.0	672	0.80	0.25	(0.35, 0.37)

[a] Device structure: ITO/PEDOT:PSS/Polymer (**6b-6d**)/LiF/Al, where the polymer (**6b-6d**) is an emitting layer, excluding **6a** because of its poor solubility.
[b] V_{on}: turn-on voltage.
[c] Φ_{EL}: external quantum yield.

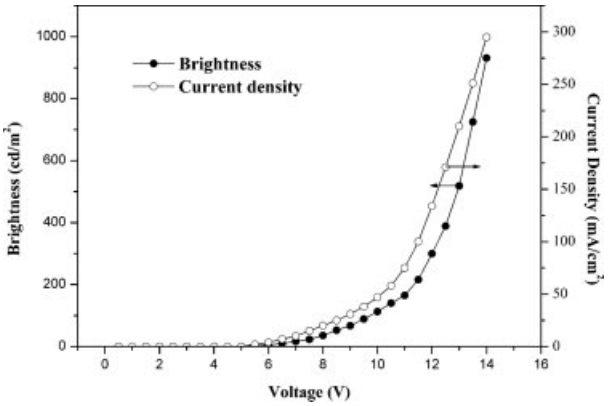

Figure 7. Current-voltage-brightness characteristics of the PLED device with the configuration of ITO/PEDOT:PSS/**6c**/LiF/Al.

coordinates, and the emission intensity was augmented by increasing bias voltages. The turn-on voltages of all devices were ~6 V, and the best power efficiency and brightness (in polymer **6c**) were 0.33 cd A^{-1} and 931 cd m^{-2} (at 14 V), respectively. The current density-voltage-brightness characteristic curves of polymer **6c** in the PLED device (device structure: ITO/PEDOT:PPS/Polymer(**6c**)/LiF/Al) are shown in Figure 7, and similar turn-on voltages for both of the current density and brightness illustrate that a matched balance of both injection and transportation in charges was achieved.[47]

Compared with the corresponding PL spectra of solid films in Figure 5 and Table 3, polymers **6c** and **6d** (excluding **6b**) both showed red shifted emissions of λ_{max} in EL spectra and polymer **6d** exhibited a broader EL emission peak (Fig. 8 and Table 4). The different EL and PL emissions of polymers **6c** and **6d** may originate from different excited state or ground states.[41] The broader EL spectra of polymer **6d** may be due to the recombination of excitons at wide interfaces of the emission layer and the hole-transporting layer in the PLED devices.[47]

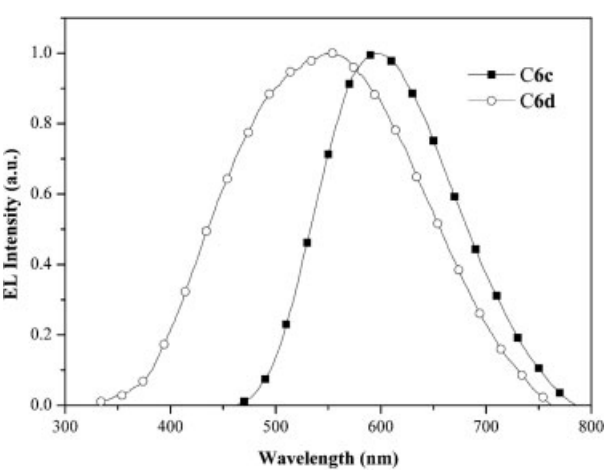

Figure 8. Normalized EL spectra of the PLED devices with the configurations of ITO/PEDOTPSS/(**6c** or **6d**)/LiF/Al.

CONCLUSIONS

In summary, a series of bistpyzinc(II)-based supramolecular polymers were obtained by self-assembled process. The formation of polymers **6a-6d** was confirmed by the increased viscosities (up to 1.5–1.83 times) relative to those of their analogous monomers. Besides, the experiments of ^{1}H NMR and UV-Vis titration over the ratio of Zn^{2+}/monomer = 1/1 confirmed the exact stoichiometric ratio of these metallo-supramolecular polymers. Various lateral substituents, such as methoxy (OMe), methyl (Me), and fluorine (F) units, were attached to the conjugated bistpy ligands, and thus to control the thermal properties and energy band gaps of the resulting metallo-polymers. Compared with the monomer counterparts, the film quality and the quantum yields of PL and EL were enhanced by the metallo-supramolecular design via introducing zinc(II) ions. These metallo-polymers gave green to yellow PL emissions (with good PL quantum yields) in solid films, and showed yellow to orange EL emissions. In general, the incorporation of lateral substituents into metallo-polymers reveals that the thermal and photophysical properties can be easily adjusted. Hence, with finely tuned structures integrated with coordination chemistry, metallo-polymers can provide a new protocol for the development of novel PLED materials.

The authors gratefully acknowledge financial support from the National Science Council of Taiwan (ROC) through NSC 93-2113*M*-009-011, and the instrumental support provided by Prof. Yu-Tai Tao (vacuum deposition) at Institute of Chemistry, Academia Sinica and Prof. Ching-Fong Shu (CV measurements) at Department of Applied Chemistry, National Chiao Tung University. (in Taiwan).

REFERENCES AND NOTES

1. Maruyama, T.; Kubota, K.; Yamamoto, T. Macromolecules 1993, 26, 4057.

2. Zhang, K.; Kumar, G. S.; Necker, D. C.; J Polym Sci Polym Chem Ed 1985, 23, 1253.
3. Barigelletti, F.; Flamigni, L.; Calogero, G.; Harmmarstrom, L.; Sauvage, J. P.; Collin, J. P. Chem Commun 1998, 7, 2333.
4. Ng, W. Y.; Chan, W. K. Adv Mater 1997, 9, 716.
5. Nguyen, P.; Gomez-Elipe, P.; Manners, I. Chem Rev 1999, 99, 1515.
6. Kalyanasundaram, K. Coord Chem Rev 1982, 46, 159.
7. El-Ghayoury, A.; Schenning, A. P. H. J.; Meijer, E. W. J Polym Sci Part A: Polym Chem 2002, 23, 957.
8. Constable, E. C. Adv Inorg Chem Radiochem 1986, 30, 69.
9. Newkome, G. R.; He, E.; Moorefield, C. N. Chem Rev 1999, 99, 1689.
10. Khlobystov, A. N.; Blake, A. J.; Champness, N. R.; Lemenkovsmii, D. A.; Majouga, A. G.; Zyk, N. V.; Schröder, M. Coord Chem Rev 2001, 222, 155.
11. Würthner, F.; Sautter, A.; Thalacker, C. Angew Chem Int Ed 2000, 39, 1243.
12. Velten, U.; Lahn, B.; Rehahn, M. Macromol Chem Phys 1997, 198, 2798.
13. Constable, E. C. Macromol Symp 1995, 98, 503.
14. Constable, E. C.; Cargill Thompson, A. M. W. J Chem Soc Dalton Trans 1992, 3467.
15. Kelch, S.; Rehahn, M. Macromolecules 1997, 30, 6185.
16. Schubert, U. S.; Eschbaumer, C. Angew Chem Int Ed 2002, 41, 2892.
17. Andres, P. R.; Schubert, U. S. Adv Mater 2004, 16, 1043.
18. Dobrawa, R.; Würthner, F. J Polym Sci Part A: Polym Chem 2005, 43, 4981.
19. Vogel, V.; Gohy, J. F.; Lohmeijer, B. G. G.; Broek, J. A. V. D.; Haase, W.; Schubert, U. S.; Schubert, D. J Polym Sci Part A: Polym Chem 2003, 41, 3159.
20. Holder, E.; Marin, V.; Alexeev, A.; Schubert, U. S. J Polym Sci Part A: Polym Chem 2005, 43, 2765.
21. Chu, Q.; Pang, Y. J Polym Sci Part A: Polym Chem 2006, 44, 2338.
22. Shunmugam, R.; Tew, G. N. J Polym Sci Part A: Polym Chem 2005, 43, 5831.
23. Tzanetos, N. P.; Andreopoulou, A. K.; Kallitsis J. K. J Polym Sci Part A: Polym Chem 2005, 43, 4838.
24. Lehn, J. M. Supramolecular Chemistry, Concepts and Perspective; VHC: Weinheim, Germany, 1995.
25. Sauvage, J. P.; Collin, J.; Chambron, J. C.; Guillerez, S.; Coudret, C.; Balzani, V.; Bargelletti, F.; De Cola, L.; Flamigni, L. Chem Rev 1994, 94, 993.
26. Yu, S. C.; Kowk, C. C.; Chan, W. K.; Che, C. M. Adv Mater 2003, 15, 1634.
27. Chang, S. C.; Bharathan, J.; Yang, Y.; Helgeson, R.; Reynolds, J. R. Appl Phys Lett 1998, 72, 2561.
28. Bliznyyuk, V. N.; Cater, S. A.; Sott, J. C.; Klarner, G.; Miller R. D.; Miller, D. C. Macromolecules 1999, 32, 361.
29. Xia, C.; Advincula, R. C. Macromolecules 2001, 34, 5854.
30. Dobrawa, R.; Lysetska, M.; Ballester, P.; Grüne, M.; Würthner, F. Macromolecules 2005, 38, 1315.
31. Chen, Y. Y.; Tao, Y. T.; Lin, H. C. Macromolecules 2006, 39, 8559.
32. Wang, X. Y.; Guzreo, A. D.; Schmehl, R. H. Chem Commun 2002, 2344.
33. Goodall, W.; Williams, J. A. G. Chem Commun 2001, 2514.
34. Lee, S. H.; Nakamura, T.; Tsutsui, T. Org Lett 2001, 33, 478.
35. Bao, Z.; Chen, Y.; Cai, R.; Yu, L. Macromolecules 1993, 26, 5281.
36. Ziener, U.; Godt, A. J Org Chem 1997, 62, 6137.
37. Potts, K. T.; Konwar, D. J Org Chem 1991, 56, 4851.
38. Ziessel, R.; Khatyr, A. J Org Chem 2000, 65, 3126.
39. Kimura, M.; Horai, T.; HanaBusa, K.; Shirai, H. Adv Mater 1998, 10, 459.
40. Heck, R. F. Org React 1982, 27, 354.
41. Iyer, P. K.; Beck, J. B.; Weder, C.; Rowan, S. J. Chem Commun 2005, 319.
42. Kowk, C. C.; Yu, S. C.; Sham, H. T.; Che, C. M. Chem Commun 2004, 2758.
43. Hu, B.; Fuchs, A.; Huseyl, S.; Gordaninejad, F. J Appl Polym Sci 2006, 100, 2464.
44. Hwang, S. H.; Wang, P.; Moorefield, C. N.; Godinez, L. A.; Manriquez, J.; Bustos, E.; Newkome, G. R. Chem Commun 2005, 4672.
45. Sung, H. H.; Lin, H. C. Macromolecules 2004, 37, 7945.
46. Huang, F.; Wu, H.; Wang, D.; Yang, W.; Cao, Y. Chem Mater 2004, 16, 708.
47. Balasubramaniam, E.; Tao, Y. T.; Danel, A.; Tomasik, P. Chem Mater 2000, 12, 2788.